International Journal of Latest Engineering and Management Research (IJLEMR)
ISSN: 2455-4847
www.ijlemr.com || REETA-2K16 ǁ PP. 17-27

A DC TO DC CONVERTER BASED NON-GRID WIND ENERGY POWER CONVERSION

T. Narasimha Reddy*, N. Sravanthi**
** Department of EEE, Vignana Bharathi Institute of Technology, Proddatur, Kadapa, A.P, India.*
*** Department of EEE, Siddartha Institute of Science and Technology, Puttur, A.P, India*

Abstract: Present energy need heavily relies on the conventional sources. But the limited availability and steady increase in the price of conventional sources has shifted the focus toward renewable sources of energy. Of the available alternative sources of energy, wind energy is considered to be one of the proven technologies. With a competitive cost for electricity generation, wind energy conversion system (WECS) is nowadays deployed for meeting both grid-connected and stand-alone load demands. However, wind flow by nature is intermittent. In order to ensure continuous supply of power suitable storage technology is used as backup. In this paper, the sustainability of a 4-kW hybrid of wind and battery system is investigated for meeting the requirements of a 3-kW stand-alone dc load representing a base telecom station. A charge controller for battery bank based on turbine maximum power point tracking and battery state of charge is developed to ensure controlled charging and discharging of battery. The mechanical safety of the WECS is assured by means of pitch control technique. Both the control schemes are integrated and the efficacy is validated by testing it with various load and wind profiles in MATLAB/SIMULNIK.

Index Terms: Maximum power point tracking (MPPT), pitch control, state of charge (SoC), wind energy conversion system (WECS).

I. INTRODUCTION

ENERGY is the considered to be the pivotal input for de-velopment. At present owing to the depletion of available conventional resources and concern regarding environmental degradation, the renewable sources are being utilized to meet the ever increasing energy demand [1]. Due to a relatively low cost of electricity production [2] wind energy is considered to be one of the potential sources of clean energy for the future [3]. But the nature of wind flow is stochastic. So rigorous testing is to be carried out in laboratory to develop efficient control strat-egy for wind energy conversion system (WECS). The study of WECS and the associated controllers are, thus, becoming more and more significant with each passing day. Nowadays, many stand-alone loads are powered by renewable source of energy. With this renewed interest in wind technology for stand-alone applications, a great deal of research is being carried out for choosing a suitable generator for stand-alone WECS. A detailed comparison between asynchronous and synchronous generators for wind farm application is made in [4]. The major advantage of asynchronous machine is that the variable speed operation allows extracting maximum power from WECS and reducing the torque fluctuations [5]. Induction generator with a lower unit cost, inherent robustness, and operational simplicity is consid-ered as the most viable option as wind turbine generator (WTG) for off grid applications [6].

However, the induction genera-tor requires capacitor banks for excitation at isolated locations. The excitation phenomenon of self-excited induction generator (SEIG) is explained in [5]–[7].

The power output of the SEIG depends on the wind flow which by nature is erratic. Both ampli-tude and frequency of the SEIG voltage vary with wind speed. Such arbitrarily varying voltage when interfaced directly with the load can give rise to flicker and instability at the load end. So, the WECS are integrated with the load by power electronic con-verters in order to ensure a regulated load voltage [8]. Again due to the intermittent characteristics of the wind power, a WECS needs to have energy storage system [9]. An analysis of the avail-able storage technologies for wind power application is made in [9] and [10]. The advantage of battery energy storage for an isolated WECS is discussed in [10]. With battery energy storage it is possible to capture maximum power [11] from the available wind. A comparison of several maximum power point tracking (MPPT) algorithms for small wind turbine (WT) is carried out in [12] and [13]. In order to extract maximum power form WECS the turbine needs to be operated at optimal angular speed [13]. However, [11] do not take into account the limit on maximum allowable battery charging current nor do they protect against battery overcharging. In order to observe the charging limita-tion of a battery a charge controller is required. Such a charge control scheme for battery charging for a stand-alone WECS using MPPT is explained in [14]. However, in this paper also the maximum battery charging current is not limited. The dis-continuous battery charging current causes harmonic heating of the battery. The terminal voltage instead of state of charge (SoC) is used for changeover from current mode to voltage mode. Also the MPPT implementation is highly parameter dependant

and will be affected by variation of these parameters with operating conditions. Moreover, as the wind speed exceeds its rated value, the WT power and speed needs to be regulated for ensuring me-chanical and electrical safety [15]. This is achieved by changing the pitch angle to the required value [16]. Several pitch control techniques are explained in [17]–[19]. The experimental result from a prototype 3-kW pitch controlled horizontal axis WT is presented in [20]. However, these references (except [20]) have considered only grid-connected systems. Even in [20], a battery storage system has not been considered. From a study of the aforementioned literature, it is observed that MPPT schemes with [14] and without [11] battery charging mode control and pitch control technique [20] have been imple-mented independently for stand-alone wind energy applications. However, none of the control strategy proposed so far has inte-grated all these three control objectives. In this paper, a hybrid wind-battery system is considered to meet the load demand of a stand-alone base telecom station (BTS).

From a study of the aforementioned literature, it is observed that MPPT schemes with [14] and without [11] battery charging mode control and pitch control technique [20] have been imple-mented independently for stand-alone wind energy applications. However, none of the control strategy proposed so far has inte-grated all these three control objectives. In this paper, a hybrid wind-battery system is considered to meet the load demand of a stand-alone base telecom station (BTS). The BTS load require-ment is modeled as a dc load which requires a nominal regulated voltage of 50 V. The WECS is interfaced with the stand-alone dc load by means of ac–dc–dc power converter to regulate the load voltage at the desired level. The proposed control scheme utilizes the turbine maximum power tracking technique with the battery SoC limit logic to charge the battery in a controlled manner. Unlike [14], the MPPT logic used here actually forces the turbine to operate at optimum TSR and hence is parameter independent. The battery charging current is always continu-ous with very low ripple thus avoiding harmonic heating. The changeover between the modes for battery charging is affected based on the actual value of the SoC. Further it also provides protection against turbine over speed, over loading, and over voltage at the rectifier output by using pitch control.

The paper is organized as follows. A brief description of the hybrid wind-battery system powering an off-gird dc load along with the power converter topology is presented in Section II. The control strategy comprising of the pitch controller for the turbine and the charge controller for the battery is discussed in Section III. The results obtained by simulating the hybrid system with different wind profiles and load variations validat-ing the efficacy of the proposed control logic are presented in Section IV. Section V concludes the paper.

II. HYBRID WIND-BATTERY SYSTEM FOR AN ISOLATED DC LOAD

The proposed hybrid system comprises of a 4-kW WECS and 400 Ah, C/10 lead acid battery bank. The system is designed for a 3-kW stand-alone dc load. The layout of the entire system along with the control strategy is shown in Fig. 1. The specifi-cations of the WT, SEIG, and battery bank are tabulated in the Appendix. The WECS consists of a 4.2-kW horizontal axis WT, gear box with a gear ratio of 1:8 and a 5.4 hp SEIG as the WTG. Since the load is a stand-alone dc load the stator terminals of the SEIG are connected to a capacitor bank for self-excitation. The ac output is rectified by three-phase uncontrolled diode rectifier. However, there is a need for a battery backup to meet the load demand during the period of unavailability of sufficient wind power. This hybrid wind-battery system requires suitable control logic for interfacing with the load. The uncontrolled dc output of the rectifier is applied to the charge controller circuit of the battery. The charge controller is a dc–dc buck converter which determines the charging and discharging rate of the battery.

The battery bank connected to the system can either act as a source or load depending on whether it is charging or discharg-ing. However, regardless of this the battery ensures that the load terminal voltage is regulated. Further, as shown in Fig. 1, the charging of the battery bank is achieved by MPPT logic, while the pitch controller limits the mechanical and electrical parameters within the rated value. The integrated action of the battery charge and pitch controller ensures reliable operation of the stand-alone WECS.

III. CONTROL STRATEGY FOR STAND-ALONE HYBRID WIND-BATTERY SYSTEM

The wind flow is erratic in nature. Therefore, a WECS is integrated with the load by means of an ac–dc–dc converter to avoid voltage flicker and harmonic generation. The control scheme for a stand-alone hybrid wind-battery system includes the charge controller circuit for battery banks and pitch control logic to ensure WT operation within the rated value. The control logic ensures effective control of the WECS against all possible disturbances.

A. Charge Controller for the Battery Bank

This section discusses in detail the development of charge controller circuit for a 400 Ah, C/10 battery bank

using a dc–dc buck converter in MATLAB/SIMULINK platform. Generally, the batteries are charged at C/20, C/10, or C/5 rates depending on the manufacturer's specification where C specifies the Ah rating of battery banks. So, the battery bank system considered in the design can be charged at 20, 40, or 80 A. But, in this paper, C/10 rate (i.e., 40 A) for battery charging is chosen. However, the current required for charging the battery bank depends on the battery SoC. A typical battery generally charges at a constant current (CC), i.e., C/10 rate mode till battery SoC reaches a certain level (90%–98%). This is referred to as CC mode of battery charging. The CC mode charges the battery as fast as possible. Beyond this SoC, the battery is charged at a constant voltage (CV) which is denoted as CV mode of battery charging in order to maintain the battery terminal voltage.

B. Control Strategy

The implementation of the charge control logic as shown in Fig. 2 is carried out by three nested control loops. The outer most control loop operates the turbine following MPPT logic with battery SoC limit. To implement the MPPT logic, the actual tip speed ratio (TSR) of turbine is compared with the optimum value. The error is tuned by a PI controller to generate the bat-tery current demand as long as the battery SoC is below the CC mode limit. Beyond this point, the SoC control logic tries to maintain constant battery charging voltage. This in turn reduces the battery current demand and thus prevents the battery bank from overcharging. The buck converter inductor current com-mand is generated in the intermediate control loop. To design the controller, it is essential to model the response of the battery current (I_b) with respect to the inductor current (I_L).

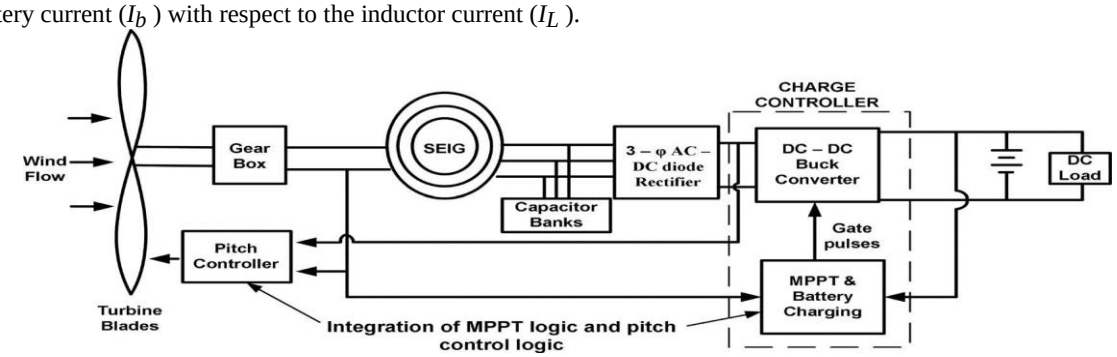

Fig. 1. Layout of hybrid wind–battery system for a stand-alone dc load.

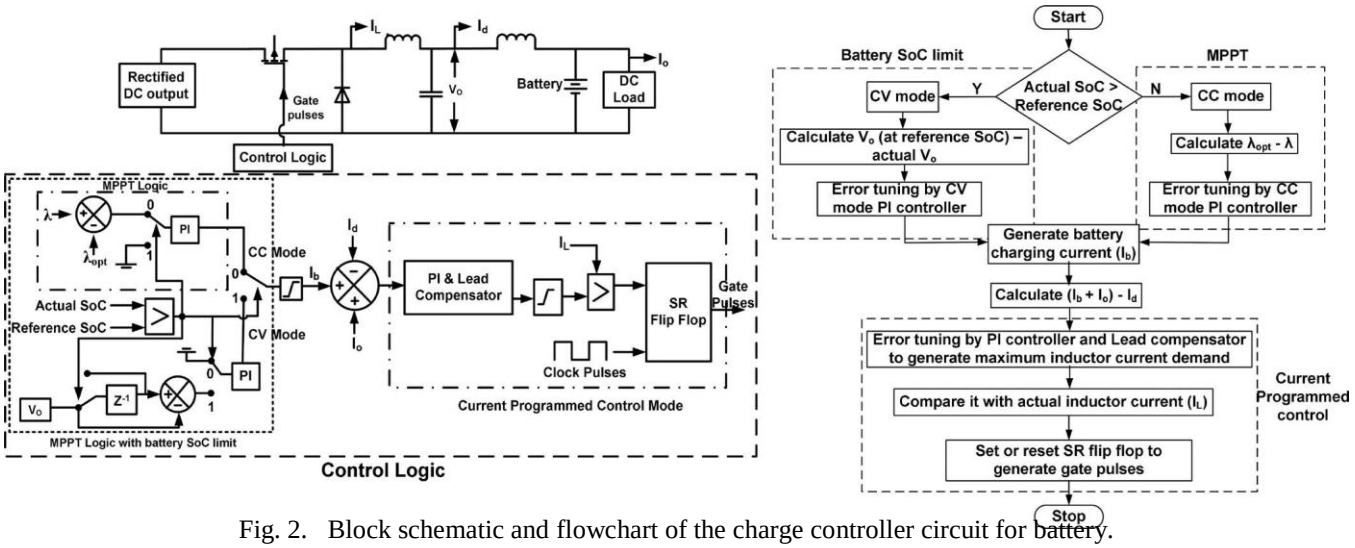

Fig. 2. Block schematic and flowchart of the charge controller circuit for battery.

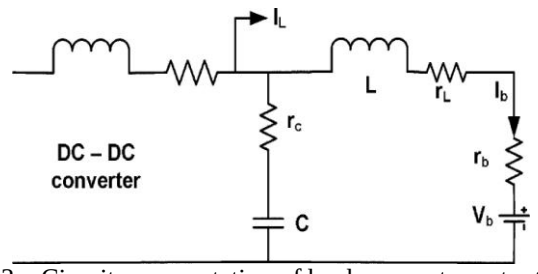

Fig. 3. Circuit representation of buck converter output.

The transfer function can be computed from Fig. 3 and is given by

$$\frac{I_b(s)}{I_L(s)} = \frac{r_c C s + 1}{LC s^2 + (r_L + r_c + r_b) C s + 1} . \quad (1)$$

As shown in Fig. 3, the battery is assumed to be a CV source with a small internal resistance (r_b). The effective series resis-tances (ESR) of the capacitor (r_c) and the inductor (r_L) are also considered. The ESR of the capacitor and the inductor is taken to be 1mΩ each. The battery internal resistance is 10 mΩ. For regulating the peak-to-peak (p–p) ripple of battery current and converter output voltage within 2% of the rated value the L and C are calculated to be 10 mH and 5 mF, respectively.

For controlling the battery current the actual converter output current (I_d) is compared with the reference (I_b + I_a) and the error is processed by a cascade of a PI and a lead compensator. The PI controller is modeled as an inverted zero. To maintain the phase margin of the open-loop system the frequency of this zero is 50 times lower than the crossover frequency. To improve the phase margin of the battery charging current control loop (i.e., (1) along with the PI controller) a lead compensator is connected in cascade with the PI controller as shown in Fig. 2.

The zero and pole of the lead compensator are designed to have a positive phase margin and to restrict the crossover fre-quency to about 14% of the switching frequency.

The bode plot of the PI controller along with the lead com-pensator and the loop gain of the battery current control loop are shown in Fig. 4(a) and (b). As shown in Fig. 4, the phase margin is 34.2° at 130 Hz. The output of the lead compensator determines inductor current reference for the dc–dc converter. In order to prevent over loading the turbine (and its consequent stalling) the lead compensator output is first passed through an adjustable current limiter. The lower limit is set to zero and the

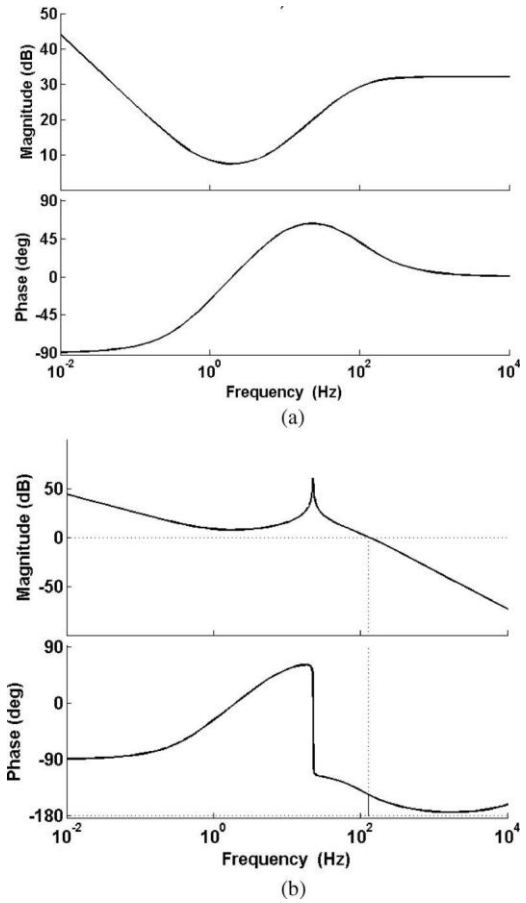

Fig. 4. Bode plot of (a) PI controller in cascade with lead compensator.
(b) Loop gain of the battery current control loop.

upper limit is varied according to the maximum power available at a given wind speed. The output of this limiter is used as the reference for the current controller in the dc–dc converter.

Finally, in the inner most loop the actual inductor current is made to track the reference using peak current mode con-trol [21]. The compensated output of the intermediate loop is compared with the instantaneous inductor current of the buck converter. The output of the comparator is applied to an SR flip-flop to produce the gate pulses for the dc–dc buck converter. The frequency of the clock pulses is 2 kHz. The frequency of the gate pulse is equal to the clock pulse frequency. This method of generating gate pulses for the converter is known as the current programmed control technique. The advantage of this method is that it does not allow the inductor current to go beyond the rated limit. This in turn protects the buck converter switch and inductor from over current situation.

IV. MODES OF BATTERY CHARGING

A. CC Mode of Battery Charging

In CC mode, the battery charging current demand is deter-mined from the MPPT logic. MPPT is implemented by com-paring the actual and optimum TSR (λ_{opt}). The error is tuned by a PI controller to generate the battery charging current as per the wind speed. In this mode, the converter output voltage rises with time while the MPPT logic tries to transfer as much power as possible to charge the batteries. The actual battery charging current that can be achieved does not remain constant but varies with available wind speed subject to a maximum of C/10 rat-ing of the battery. The battery charging current command has a minimum limit of zero. In case the wind speed is insufficient to supply the load even with zero battery charging current the inductor current reference is frozen at that particular value and the balance load current is supplied by the battery.

B. CV Mode of Battery Charging

In the CC mode, the battery voltage and SoC rise fast with time. However, the charge controller should not overcharge the batteries to avoid gasification of electrolyte [14]. As a result, once the battery SoC becomes equal to the reference SoC the controller must switch over from CC mode to CV mode. In CV mode, the battery charging voltage is determined from the buck converter output voltage (V_O). The value of the converter volt-age when the battery SoC reaches 98% is set as the reference value and is compared with the actual converter output volt-age. The error in the voltage is then controlled by a cascaded arrangement of PI controller and lead compensator to generate the inductor current reference. It is then compared with the ac-tual inductor current by a logical comparator to generate gate pulses in a similar way as described in Section A. In this mode, the converter output voltage is maintained at a constant value by the controller action. So, in CV mode the battery voltage and SoC rise very slowly with time as compared to CC mode. The battery charging current slowly decreases with time, since the potential difference between the buck converter output and battery terminal gradually reduces.

Thus, in CC mode the buck converter output current is regu-lated while the output voltage keeps on increasing with time. On the contrary in CV mode the output voltage is regulated, while the current in the circuit reduces gradually. To study the CC and CV mode of battery charging, rated value of wind speed is applied to the system. The battery parameters and the converter output parameters are observed with time. The results are shown in Fig. 5.

As shown in Fig. 5, the battery is charged both in CC mode and CV mode. The transition from CC to CV mode takes place when the battery SoC reaches 98%. This is because in the present design, the threshold SoC for switch over in the control logic is set at 98%. As discussed in the earlier section, in the CC mode the battery charges at a CC of 40 A which is the C/10 value for a 400-Ah battery bank. During this mode, both converter output voltage and battery voltage rise. The battery SoC rises from an initial SoC level of 97.95% to 98% within 17 s. As the battery reaches the threshold SoC level, the buck converter voltage is regulated by the controller action at a constant value of 53 V while the converter current gradually reduces from 40 A at 17 s to 10 A at 40 s. The battery SoC slowly rises from 98% to 98.03%. The results indicate that the battery charges at a faster rate in CC mode as compared to CV mode. Thus, in CC mode much of the available power from primary source is injected into

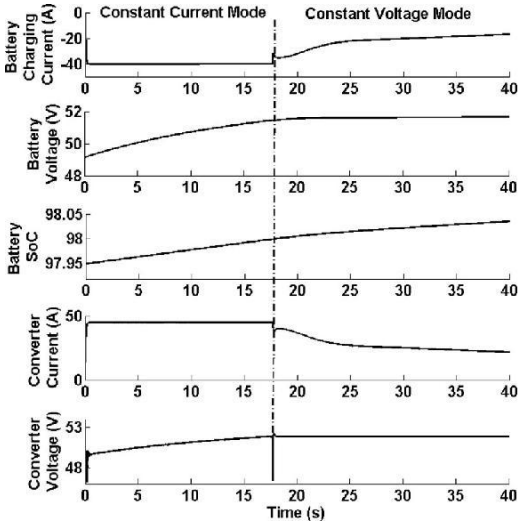

Fig. 5. Battery charging modes at a constant wind speed of 10 m/s.

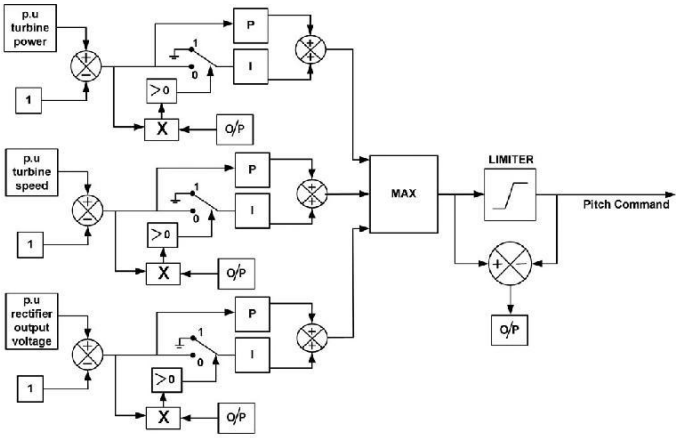

Fig. 7. Pitch control scheme for a stand-alone WECS.

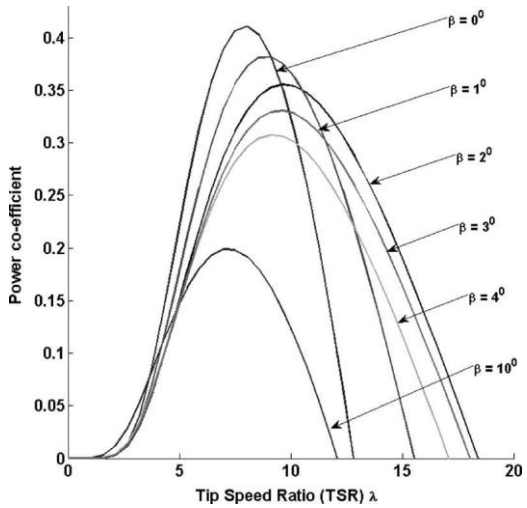

Fig. 6. $C_p - \lambda$ characteristics of the WT for different pitch angles.

the battery whereas in CV mode the battery is charged slowly to avoid gasification and heating issue.

C. Pitch Control Mechanism

The WT power output is proportional to the cube of wind velocity [15]. Generally the cut-off wind speed of a modern WT is much higher compared to the rated wind speed [9]. If the WT is allowed to operate over the entire range of wind speed without implementation of any control mechanism, the angular speed of the shaft exceeds its rated value which may lead to damage of the blades. So, it is very much essential to control the speed and power at wind speeds above the rated wind speed. This is achieved by changing the pitch angle of the blade. Such a mechanism is referred to as the pitch control of WT.

The power coefficient (C_p) versus TSR (λ) characteristics of the WT considered in this study for different pitch angles are shown in Fig. 6. As examined from the characteristics, at a pitch angle of zero degree the value of C_p is maxima. But the optimum value of power coefficient reduces with increase in pitch angle. This happens because with increase in blade pitch the lift coefficient reduces which results in decreasing the value of C_p [15]. So, the pitch control mechanism controls the power output by reducing the power coefficient at higher wind speeds. Below the rated wind speed the blade pitch is maintained at zero degree to obtain maximum power. The pitch controller increases the blade pitch as the WT parameters exceed the rated value. The reduction in the value of C_p by pitching compensates for the increase in WT power output under the influence of higher wind speeds. Apart from

regulating the WT parameters, it is also essential to control the output voltage of the ac–dc rectifier to avoid overvoltage condition in the WECS. Hence, the pitch controller ensures that with desirable pitch command, the WT parameters and the rectifier output dc voltage are regulated within their respective maximum allowable limits to ensure safe operation of the WECS.

D. Pitch Control Scheme

The pitch control scheme is shown in Fig. 7. As seen the p.u. value of each input is compared with 1 to calculate the error. The errors are tuned by PI controller. The "MAX" block chooses the maximum output from each PI controller which is then passed on to a limiter to generate the pitch command for the WT. The actual pitch command is compared with the limited value. The lower limit of the pitch command is set at zero. There arises an error when the actual pitch command goes above or below the specified limit. This is multiplied with the error obtained from each of the comparator. The product is compared with zero to determine the switching logic for integrator. This technique is carried out to avoid integrator saturation. The pitch controller changes the pitch command owing to variation in turbine rotation speed, power, and output voltage of rectifier, which ensures safe operation of the WECS.

V. RESULTS AND DISCUSSIONS

A WECS needs to be efficient to ensure continuous power flow to the load. The effectiveness can be achieved by integrating the hybrid wind-battery system with suitable control logic. This includes the charge control logic and the pitch control logic. The charge controller regulates the charging and discharging

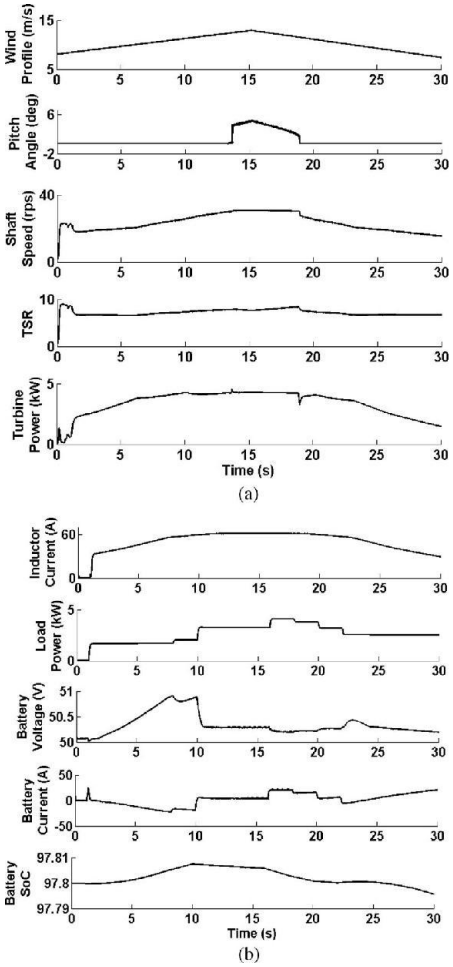

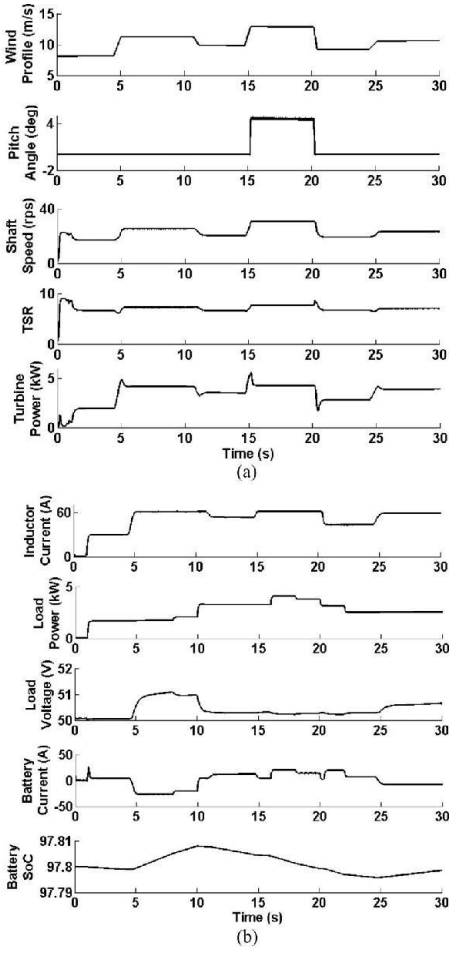

Fig. 8. (a) WT and (b) battery parameters under the influence of gradual variation of wind speed.
Fig. 9. (a) WT and (b) battery parameters under the influence of step variation of wind speed.

rate of the battery bank while the pitch controller controls the WT action during high wind speed conditions or in case of a power mismatch. Both the control strategy are integrated with the hybrid system and simulated with various wind profiles to validate the efficacy of the system. The system is connected to a load profile varying in steps from 0 to 4 kW. The WT parameters like shaft speed, TSR, blade pitch and output power are analyzed with variation in wind speed conditions. The current profile of the converter, load, and the battery are also monitored with the wind profile. To ensure uninterrupted power flow, load demand is given more priority over battery charging. The WT and battery parameters are observed for the following wind profiles.

1) Gradual rise and fall in wind speed.

2) Step variation in wind speed.

3) Arbitrary variation in wind speed.

A gradual rise and fall in wind speed as shown in Fig. 8(a) is applied to the WT. The wind speed gradually rises from 8 to 12 m/s in 15 s and then falls to 8 m/s in the next 15 s. The WT parameters and the current profile of the converter, load and the battery are observed in Fig. 8(a) and (b). Further the efficacy of the complete control scheme is validated with a step variation in wind profile and an arbitrary varying wind speed. The variation of the wind profile in step from 8 to 12 m/s is shown in Fig. 9(a) while the arbitrary variation in wind speed from 6 to 14 m/s is highlighted in Fig 10(a). The response of WT parameter and the current profiles with respect to step variations and arbitrary variations are shown in Figs. 9 and 10, respectively. The results also demonstrate the change in battery SoC for all possible wind profiles.

From Figs 8–10, it is observed, that when the wind speed is below the rated value (10 m/s) the MPPT scheme regulates the TSR of WT at its optimum value irrespective of the variation in wind profile. Thus maximum power is extracted from WECS at all wind speeds to meet the load requirement and charge the battery bank. But, the wind power is not always sufficient to meet the load demand and charge the battery in CC mode. In such situations the system first meets the load requirement and charges the battery bank at a reduced rate. Moreover, when the wind-battery system is chosen to supply the desired load power. To mitigate the random characteristics of wind flow the WECS is interfaced with the load by suitable controllers. The control logic implemented in the hybrid set up includes the charge con-trol of battery bank using MPPT and pitch control of the WT for assuring electrical and mechanical safety. The charge con-troller tracks the maximum power available to charge the battery bank in a controlled manner. Further it also makes sure that the batteries discharge current is also within the C/10 limit. The cur-rent programmed control technique inherently protects the buck converter from over current situation. However, at times due to MPPT control the source power may be more as compared to the battery and load demand. During the power mismatch con-ditions**,** the pitch action can regulate the pitch angle to reduce the WT output power in accordance with the total demand. Be-sides controlling the WT characteristics, the pitch control logic guarantees that the rectifier voltage does not lead to an over-voltage situation. The hybrid wind-battery system along with its control logic is developed in MATLAB/SIMULINK and is tested with various wind profiles. The outcome of the simulation experiments validates the improved performance of the system

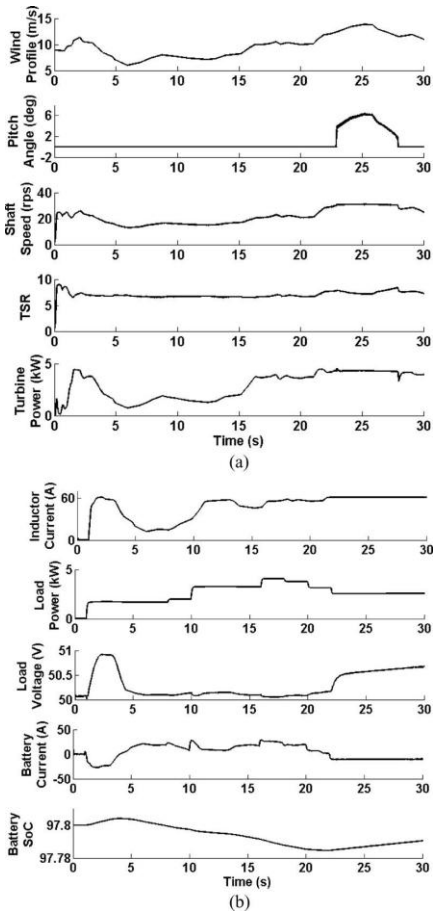

Fig. 10. (a) WT and (b) battery parameters under the influence of arbitrary variation of wind speed.

APPENDIX

TABLE I
WT SYSTEM SPECIFICATIONS

Parameters	Value (units)
Rated power	4000 W
Radius	2.3 m
Cut-in wind speed	4 m/s
Rated wind speed	10 m/s
Inertia co-efficient	7 kgm^2
Optimum Tip speed ratio	7
Optimum power co-efficient	0.41

TABLE II
SQUIRREL CAGE INDUCTION MACHINE SPECIFICATIONS

Parameters	Value (units)
Rated Power	5.4 hp
Stator resistance	2.6 Ω
Stator leakage inductance	4 mH
Mutual inductance	240 mH
Rotor resistance	2 Ω
Rotor leakage inductance	4 mH
Excitation capacitance (at full load) connected in Δ	15 μF

wind power is not adequate as per the load demand, the battery discharges to meet the deficit. The battery SoC increases during charging but decreases while discharging. However, the charge controller ensures that the battery current during charging or discharging never exceeds 40 A. The pitch angle of WT is maintained at zero deg at wind speed below 10 m/s. But the pitch controller is activated as the wind speeds exceeds its rated limit. The increase in the pitch angle limits the power and speed output within the safe limits of WT operation. The response of WT and currents for all possible variations in wind profile indeed prove the efficacy of the proposed control logic for the hybrid wind–battery system.

TABLE III
BATTERY SPECIFICATIONS

Parameters	Value (units)
Ampere hour rating	400 Ah
Nominal Voltage	48 V
Fully charged Voltage (No load)	55.2 V
Charging rate	C/10

VI. CONCLUSION

The power available from a WECS is very unreliable in na-ture. So, a WECS cannot ensure uninterrupted power flow to the load. In order to meet the load requirement at all instances, suit-able storage device is needed. Therefore, in this paper, a hybrid

REFERENCES

[1] A. D. Sahin, "Progress and recent trends in wind energy," *Progress in Energy Combustion Sci.*, vol. 30, no. 5, pp. 501–543, 2004.
[2] R. D. Richardson and G. M. Mcnerney, "Wind energy systems," *Proc. IEEE*, vol. 81, no. 3, pp. 378–389, Mar. 1993.
[3] R. Saidur, M. R. Islam, N. A. Rahim, and K. H. Solangi, "A review on global wind energy policy," *Renewable Sustainable Energy Rev.*, vol. 14, no. 7, pp. 1744–1762, Sep. 2010.
[4] M. T. Ameli, S. Moslehpur, and A. Mirzale, "Feasibility study for replac-ing asynchronous genrators with synchronous generators in wind farm power stations," in *Proc. IAJC – IJME, Int. Conf. Eng. Technol.*, Music City Sheraton, Nashville, TN, US, ENT paper 129Nov. 17–19, 2008.
[5] G. K. Singh, "Self excited generator research—A survey," *Electric Power Syst. Res.*, vol. 69, no. 2/3, pp. 107–114, 2004.
[6] R. C. Bansal, "Three-phase self-excited induction generators: An overview," *IEEE Trans. Energy Convers.*, vol. 20, no. 2, pp. 292–299, Jun. 2005.
[7] S. C. Tripathy, M. Kalantar, and N. D. Rao, "Wind turbine driven self excited induction generator," *Energy Convers. Manag.*, vol. 34, no. 8, 641–648, 1993.
[8] A. Chakraborty, "Advancements in power electronics and drives in inter-face with growing renewable energy resources," *Renewable Sustainable Energy Rev.*, vol. 15, no. 4, pp. 1816–1827, May 2011.
[9] F. D. Gonzalez,´ A. Sumper, O. G. Bellmunt, and R. V. Robles, "A review of energy storage technologies for wind power applications," *Renewable Sustainable Energy Rev.*, vol. 16, no. 4, pp. 2154–2171, May 2012.
[10] N. S. Hasan, M. Y. Hassan, M. S. Majid, and H. A. Rahman, "Review of storage schemes for wind energy systems," *Renewable Sustainable Energy Rev.*, vol. 21, pp. 237–247, May 2013.
[11] A. M. D. Broe, S. Drouilhet, and V. Gevorgian, "A peak power tracker for small wind turbines in battery charging applications," *IEEE Trans. Energy Convers.*, vol. 14, no. 4, pp. 1630–1635, Dec. 1999.
[12] R. Kot, M. Rolak, and M. Malinowski, "Comparison of maximum peak power tracking algorithms for a small wind turbine," *Math. Comput. Simul.*, vol. 91, pp. 29–40, 2013.
[13] M. Narayana, G. A. Putrus, M. Jovanovic, P. S. Leung, and S. McDonald, "Generic maximum power point tracking controller for small-scale wind turbines," *Renewable Energy*, vol. 44, pp. 72–79, Aug. 2012.
[14] K. Y. Lo, Y. M. Chen, and Y. R. Chang, "MPPT battery charger for stand-alone wind power system," *IEEE Trans. Power Electron.*, vol. 26, no. 6, pp. 1631–1638, Jun. 2011.
[15] E. Hau, *Wind Turbines Fundamentals, Technologies, Application, Eco-nomics*, 2nd ed. New York, NY, USA: Springer, Dec. 2005.
[16] H. Camblong, "Digital robust control of a variable speed pitch regulated wind turbine for above rated

wind speeds," *Control Eng. Practice*, vol. 16, no. 8, pp. 946–958, Aug. 2008.

[17] E. Muljadi and C. P. Butterfield, "Pitch-controlled variable-speed wind turbine generation," *IEEE Trans. Ind. Appl.*, vol. 37, no. 1, pp. 240–246, Jan./Feb. 2001.

T.Narasimha Reddy received the B.Tech. degree in Electrical and Elctronics Engineering from Sri Venkatesa Perumal College of Engineering and Technology Puttur, AP, India, in 2009, and the M.Tech degree in Electrical Power Systems from St.Mary's Group of institutions Hyderabad, T.S, India, in 2015, where he is currently working as a Assistant Professor in Vignana Bharathi Institute of Technology, Proddatur, kadapa, A.P, India. His research interest includes the area of power and energy systems. Email:narasimha.vbtk@gmail.com

N.Sravathi received the B.Tech. degree in Electrical and Elctronics Engineering from Sri Venkatesa Perumal College of Engineering and Technology Puttur, AP, India, in 2009, and the M.Tech degree in Power Electronics and Electrical Drives from Sri Venkatesa Perumal College of Engineering and Technology Puttur, AP, India, in 2013, where she is currently working as a Assistant Professor in Siddartha Institute of Science and Technology, Puttur, A.P, India. Her research interest includes the area of power electronics and electrical drives.
Email: sravanthireddy224@gmail.com